

Magnetic Field Evolution of White Dwarfs in Strongly Interacting Binary Star Systems

Adrian T. Potter and Christopher A. Tout

University of Cambridge, Institute of Astronomy, The Observatories, Madingley Road, Cambridge CB3 0HA

3 November 2018

ABSTRACT

The surface magnetic field strength of white dwarfs is observed to vary from very little to around 10^9 G. Here we examine the proposal that the strongest fields are generated by dynamo action during the common envelope phase of strongly interacting stars that leads to binary systems containing at least one white dwarf. The resulting magnetic field depends strongly on the electrical conductivity of the white dwarf, the lifetime of the convective envelope and the variability of the magnetic dynamo. We assess the various energy sources available and estimate necessary lifetimes of the common envelope. In the case of a dynamo that leads a randomly oriented magnetic field we find that the induced field is confined to a thin boundary layer at the surface of the white dwarf. This then decays away rapidly upon dispersal of the common envelope. The residual field is typically less than 10^{-8} times the strength of the external field. Only in the case where there is some preferential direction to the dynamo-generated field can an induced field, that avoids rapid decay, be produced. We show that a surface field of magnitude a few per cent of the external field may be produced after a few Myr. In this case the residual field strength is roughly proportional to the lifetime of the dynamo activity.

1 INTRODUCTION

Surveys of the galactic white dwarf (WD) population have discovered magnetic field strengths ranging up to about 10^9 G (Schmidt et al. 2003). Typically WDs fall into two categories, those with field strengths of the order 10^6 G or higher and those with fields weaker than around 10^5 G. We focus here on highly magnetic WDs (hereinafter MWDs) with field strengths greater than 10^6 G. Landstreet & Angel (1971) proposed a fossil field mechanism based on the evolution of Ap/Bp stars but it is difficult to argue that such a field can survive stellar evolution in which all parts of the star have passed through convective phases. Here we build on the proposal of Tout et al. (2008) that the origin of such fields lies in the interaction between the WD and its companion star in a binary system.

This assertion is based on observations from the SDSS that approximately 10 per cent of isolated WDs are highly magnetic (Liebert et al. 2005) as are 25 per cent in cataclysmic variables (Wickramasinghe & Ferrario 2000) while there are none to be found in wide detached binary systems. Of the 1253 binary systems comprising a WD and non-degenerate M-dwarf star surveyed in the SDSS Data Release Five (Silvestri et al. 2007) none have been identified with magnetic fields greater than the detection limit of about 3 MG. The relatively high occurrence of MWDs in strongly interacting binaries compared with elsewhere suggests that the generation of the strong magnetic fields is likely the result of the interaction and subsequent evolution of the binary system. The MWDs observed in isolated systems may be explained by either the total disruption of the companion star during unstable mass transfer or the coalescence of the MWD and the core of its companion following loss of sufficient orbital energy to the common envelope (hereinafter CE) or via gravitational radiation.

When a giant with a degenerate core expands beyond its Roche Lobe mass transfer may proceed on a dynamical time scale. A dense, typically main-sequence star, companion cannot accrete the overflowing material fast enough so that it instead swells up to form a giant CE. As a result of energy transfer and angular momentum to the CE during orbital decay of the dense companion and the remnant core, strong differential rotation is established within the envelope. Also, owing to its size and thermal characteristics together with the nuclear energy source at the core, the CE is expected to be largely convective. In the mechanism proposed by Tout et al. this is expected to drive strong dynamo action giving rise to powerful magnetic

arXiv:0911.3657v1 [astro-ph.SR] 18 Nov 2009

fields (Regös & Tout 1995; Tout & Pringle 1992). If sufficiently strong dynamo action occurs in the CE then comparable magnetic fields may be induced in the degenerate core (DC) that will evolve into a WD once the envelope has been removed. We show here that strong surface fields can result from CE evolution. The strength of such fields is highly dependent on the electrical conductivity of DC, the lifetime of the CE and the variability of the magnetic dynamo.

In section 2 we outline the various sources of energy in the binary/CE system and their relation to the energy requirements of the magnetic dynamo. In section 3 we discuss the governing equations of the system and derive the form of the magnetic field for a general spatially and temporally varying magnetic diffusivity $\eta(\mathbf{r}, t)$ via the static induction equation. Then in section 4 we give an overview of the numerical methods we have used to solve the various stages of the problem. In section 5 we present our results and we discuss these and conclude in section 6.

2 CE EVOLUTION AND ENERGY CONSTRAINTS

In the absence of detailed hydrodynamic properties, the most favoured models for common envelope evolution are the so-called α (Webbink 1976; Livio & Soker 1988) and γ (Paczynski & Ziółkowski 1967; Nelemans et al. 2000) prescriptions which use a one dimensional parametrization of the transfer of energy and angular momentum respectively between the binary orbit and the envelope. We consider the energy content of a typical envelope compared to the energy necessary to generate the desired magnetic fields.

The primary sources of energy in the CE are the orbital energy of the binary system itself and the gravitational binding energy of the envelope. In the α prescription, energy is transferred from the orbit to the envelope and this leads to the expulsion of the envelope and decay of the orbital separation. This is regarded as the most likely origin of cataclysmic variables (Paczynski 1976; Meyer & Meyer-Hofmeister 1979). Other potential sources are the thermal energy content of the envelope and its rotational energy. However for a virialised cloud, these energies are small compared to the other energy sources. In some systems recombination energy can be similar in magnitude to the binding energy so may become important (Webbink 2008).

Let W , O and M be the binding, orbital and magnetic energy content of the binary/CE system respectively.

$$W = \eta_w \frac{GM_{\text{env}}M_{\text{T}}}{R_{\text{env}}}, \quad (1)$$

$$O = \frac{GM_c M_2}{a}, \quad (2)$$

and

$$M = \frac{B^2}{2\mu_0}(2\pi a)(\pi r_1^2), \quad (4)$$

where M_{env} is the mass of the CE with radius R_{env} , M_c is the mass of the degenerate core, M_2 is the mass of the dense companion, η_w is a constant of order unity that might be estimated from stellar models. The total mass of the system is $M_{\text{T}} = M_{\text{env}} + M_c + M_2$ and a is the final orbital separation. As we would expect, the total available energy is less than the energy required to produce a field of the desired strength throughout the cloud. However, given that we anticipate that the field is generated by dynamo action, the strongest fields occur where the hydrodynamic motions of the CE are most strongly perturbed. We imagine this region to be a torus of the orbital radius a and cross-sectional radius r_1 which is a few times $\max(R_2, R_c)$ where R_2 is the radius of the dense companion and R_c is the radius of the core of the giant. The energy of the cloud is then approximated by

$$W = 4.6 \times 10^{38} \eta_w \left(\frac{M_{\text{env}}}{M_{\odot}}\right) \left(\frac{M_{\text{T}}}{2.6 M_{\odot}}\right) \left(\frac{R_{\text{env}}}{10 \text{ au}}\right)^{-1} \text{ J}, \quad (5)$$

$$O = 1.0 \times 10^{41} \left(\frac{M_c}{0.6 M_{\odot}}\right) \left(\frac{M_2}{M_{\odot}}\right) \left(\frac{a}{0.01 \text{ au}}\right)^{-1} \text{ J}, \quad (6)$$

and

$$M = 5.7 \times 10^{39} \left(\frac{B}{10^7 \text{ G}}\right)^2 \left(\frac{a}{0.01 \text{ au}}\right) \left(\frac{r_1}{R_{\odot}}\right)^2 \text{ J}. \quad (8)$$

Most of the energy may be derived from the orbital decay of the binary within the CE. The value of a we have taken is for a typical separation with orbital period of 1 d and thus represents the final separation of the system. As the orbit decays, the increase in orbital velocity results in stronger local perturbations to the CE and in an increase in dynamo activity that produces stronger magnetic fields provided the CE is still sufficiently dense around the stellar cores. Therefore it is more appropriate to consider the late stage of CE evolution from the point of view of magnetic dynamos.

For the AM Herculis system $M_c = 0.78 M_\odot$ (Gänsicke et al. 2006), $M_2 = 0.37 M_\odot$ (Southwell et al. 1995), $a = 1.1 R_\odot$ (Kafka et al. 2005) and $B = 1.4 \times 10^7$ G (Wickramasinghe & Martin 1985). Taking $M = O$ gives $r_1 = 2.1 (B/10^9 \text{ G})^{-1} R_\odot$. This represents the limiting radius in which a field of sufficient strength were generated given the total energy available. This is far larger than the radius of the DC and somewhat larger than the second star and so energetically there is nothing to prevent the necessary field from being generated.

3 GOVERNING EQUATIONS FOR MAGNETIC FIELD EVOLUTION

Consider the system evolving according to the static induction equation for a general isotropic magnetic diffusivity field, $\eta(\mathbf{r}, t)$, related to the electrical conductivity, σ by $\eta = \frac{c^2}{4\pi\sigma}$. The DC is embedded in an infinite, uniform, vertical, time dependent magnetic field. This is a sensible approximation provided the length scale for variation of the external field defined by the dynamo action in the CE is sufficiently large compared to the radius of the DC. We expect the DC to be spherically symmetric and we further assume the external field to be locally axisymmetric at the surface of the DC. In reality the exact form of the imposed field is uncertain and is likely to support a complex geometry. This is supported by spectropolarimetric observations of WD magnetic field morphologies (Valyavin et al. 2006). We consider what effect this might have later on.

Except where explicitly stated otherwise, we are working in spherical polar coordinates (r, θ, ϕ) . Outside of the DC ($r > r_c$) we require

$$\nabla \times \mathbf{B} = \mathbf{0} \quad (9)$$

and

$$\mathbf{B} \rightarrow B_z(t) \mathbf{e}_z \quad \text{as } r \rightarrow \infty. \quad (10)$$

Equation (9) is satisfied locally around the DC because the magnetic field is a superposition of the curl-free imposed field and the dipole field produced by the DC. In the global field we expect this condition to be broken to the motions of the CE. Inside the DC the magnetic field evolves according to the MHD induction equation with stationary fluid,

$$\frac{d\mathbf{B}}{dt} = \nabla \times (\eta \nabla \times \mathbf{B}). \quad (11)$$

We have ignored the term $\nabla \times (\mathbf{u} \times \mathbf{B})$, assuming that this term, that results from fluid motions within the DC, is dominated by the diffusive term. If this term were large then we would expect WDs to support dynamo action. This is not supported by the statistics presented in section 1. The magnetic field must be continuous at $r = r_c$. We proceed by decomposing the magnetic field into poloidal and toroidal parts

$$\mathbf{B} = \nabla \times (T\mathbf{r}) + \nabla \times (\nabla \times (S\mathbf{r})), \quad (12)$$

where the first term on the right is the toroidal part of the magnetic field and the second term is the poloidal part. In the case of the magnetic field external to the DC, equation (9) simplifies to

$$\mathcal{L}^2 T = 0, \quad \text{and} \quad \mathcal{L}^2 (\nabla^2 S) = 0, \quad (13)$$

where

$$\mathcal{L}^2 = - \left\{ \frac{1}{\sin \theta} \frac{\partial}{\partial \theta} \left[\sin \theta \frac{\partial}{\partial \theta} \right] + \frac{1}{\sin^2 \theta} \frac{\partial^2}{\partial \phi^2} \right\}. \quad (14)$$

Taking $S = \sum_{l=1}^{\infty} S_l(r, t) P_l(\cos \theta)$ (similarly for T) and given $\mathcal{L}^2 P_l(\cos \theta) = l(l+1) P_l(\cos \theta)$ this implies

$$T = 0, \quad \nabla^2 S = 0. \quad (15)$$

The condition $\mathbf{B} \rightarrow B_z \mathbf{e}_z$ is equivalent to $S \rightarrow \frac{1}{2} B_z r \cos \theta$. The solutions of $\nabla^2 S = 0$ give S in terms of spherical harmonics. In the far-field the only mode is that corresponding to $l = 1$. The other modes decay exponentially without some mechanism to regenerate them. Thus we take S outside of the DC to be of the form

$$S = \left(S_0(t) r^{-2} + \frac{1}{2} B_z(t) r \right) \cos \theta. \quad (16)$$

where $B_z(t)$ is the external field arising from the dynamo activity in the CE. Now consider the field inside the DC. Provided the magnetic diffusivity is spherically symmetric we can again decompose \mathbf{B} into poloidal and toroidal parts to see that S and T evolve according to

$$\dot{S} = \eta(r, t) \nabla^2 S \quad \text{and} \quad \dot{T} = \eta(r, t) \nabla^2 T. \quad (17)$$

If we assume that we may write the diffusivity in the self-similar form $\eta(r, t) = \eta_r(r) \eta_t(t)$ then the equation is completely separable. So suppose we write $T(\mathbf{r}, t) = U(t) V(\mathbf{r})$ then we find that the two functions satisfy

$$\frac{\dot{U}}{\eta_t U} = \frac{\eta_r \nabla^2 V}{V} = -\lambda^2, \quad \text{where } \lambda \text{ is a complex constant} \quad (18)$$

so that

$$U = \exp\left(-\lambda^2 \int \eta_t(t) dt\right) \quad (19)$$

and

$$\nabla^2 V + \frac{\lambda^2}{\eta_r} V = 0. \quad (20)$$

In the case of spatially constant diffusivity, equation (20) is simply Helmholtz' equation. Choosing solutions which are bounded as $r \rightarrow 0$ gives solutions of the form $V \propto j_1(ar) \cos \theta$ where j_i represents the i^{th} spherical Bessel function of the first kind and $a = \sqrt{\frac{\lambda^2}{\eta_r}}$. In order to satisfy continuity in the magnetic field at $r = r_c$ we must have $j_1(ar_c) = 0$. This gives a real value of a and so λ must be real. So with no way to replenish the toroidal field, $T \rightarrow 0$ exponentially by equation (19).

It should be noted that although we have assumed that all higher order spherical harmonics, azimuthal modes of the toroidal magnetic field decay exponentially we have not presented here additional consideration to the relative decay times. Given the vertical form of the imposed external field, the dipole mode is the only one induced by the CE and therefore the only mode we focus on. A similar analysis may be performed for other values of l but these modes are only important if they are produced by the external field.

The equation for S can be treated in a very similar way to T . For $r < r_c$ we write

$$S = \int_{-\infty}^{\infty} R(r; \gamma) \exp(i\gamma H) \cos \theta d\gamma. \quad (21)$$

By taking $H = \int \eta_t(t) dt$ the system is reduced to a Fourier analysis. It is possible to use different transform methods with different choices of the parameter γ . However, because we shall consider an oscillating external field, this is the natural choice. In this form the function is still separable and R solves the equation

$$\nabla^2(R \cos \theta) = \frac{i\gamma}{\eta_r} R \cos \theta \quad (22)$$

so that

$$\frac{d^2 R}{dr^2} + \frac{2}{r} \frac{dR}{dr} - \left(\frac{i\gamma}{\eta_r} + \frac{2}{r^2}\right) R = 0. \quad (23)$$

In order to enforce continuity at the boundary we must have S and $\frac{\partial S}{\partial r}$ continuous at $r = r_c$ for all θ . These are equivalent to

$$\int_{-\infty}^{\infty} \frac{\partial R(r; \gamma)}{\partial r} \Big|_{r=r_c} \exp(i\gamma H) d\gamma = -\frac{2S_0(t)}{r_c^3} + \frac{1}{2} B_z(t) \quad (24)$$

and

$$\int_{-\infty}^{\infty} R(r_c, \gamma) \exp(i\gamma H) d\gamma = \frac{S_0(t)}{r_c^2} + \frac{1}{2} B_z(t) r_c. \quad (25)$$

By taking $\frac{1}{3}((25) - r_c(24))$ and $\frac{4}{3}((25)/r_c + \frac{1}{2}(24))$ these become

$$\frac{1}{3} \int_{-\infty}^{\infty} \left(R(r_c, \gamma) - \frac{\partial R(r; \gamma)}{\partial r} \Big|_{r=r_c} r_c \right) \exp(i\gamma H) d\gamma = \frac{S_0(H)}{r_c^2} \quad (26)$$

and

$$\frac{4}{3} \int_{-\infty}^{\infty} \left(\frac{R(r_c, \gamma)}{r_c} + \frac{1}{2} \frac{\partial R(r; \gamma)}{\partial r} \Big|_{r=r_c} \right) \exp(i\gamma H) d\gamma = B_z(H). \quad (27)$$

We take $\mathbf{B}(H(t))$ as given and so focus for the moment on the second of these equations. This allows us to solve for S and then we can derive the magnetic field within the DC. So if the transform of $B_z(H)$ is $\hat{B}_z(\gamma)$ then we may rewrite the previous equation as

$$\hat{B}_z(\gamma) = \frac{4}{3} \left(\frac{R(r_c; \gamma)}{r_c} + \frac{1}{2} \frac{\partial R(r; \gamma)}{\partial r} \Big|_{r=r_c} \right). \quad (28)$$

So given the condition $R \rightarrow 0$ as $r \rightarrow 0$ and this boundary condition we can now fully determine R . This in turn fully solves the internal (and external) dipole field of the DC. In the case $T = 0$, $S = Q(t)R(r) \cos \theta$, the internal magnetic field (for a particular γ) is given by

$$\mathbf{B} = Q(t) \left(2 \frac{R}{r} \cos \theta \mathbf{e}_r - \left(\frac{R}{r} + \frac{\partial R}{\partial r} \right) \sin \theta \mathbf{e}_\theta \right). \quad (29)$$

In theory we may solve this system exactly for any imposed field. However, owing to the complexity of the external field and its Fourier transform under the change of variable $t \rightarrow H(t)$, numerical computations become extremely difficult. Thus, for the most part, we focus on single modes given by some specific γ . This is ultimately justified by the slow variation of η during the lifetime of the CE.

In the case where the induced magnetic field is not entirely dipolar, the final term in equation (23) is modified by some factor for each l . In the case of uniform diffusivity this gives spherical Bessel functions of varying order. The forms of these functions in this parameter regime are actually very similar to the first order function considered in section 5 so we do not expect including the higher modes to affect the qualitative results significantly for the overall strength and radial variation of the internal field. In addition, given the uncertainties regarding the geometry of the magnetic field of the CE, inclusion of higher order harmonics is unlikely to give any better insight.

4 NUMERICAL METHODS

We calculated the spatial form of the magnetic field in the presence of an oscillating external field with a sixth order adaptive step Runge-Kutta algorithm (Press et al. 1992) according to equation (29). The equation was integrated from the centre out to the surface with boundary conditions $R(0) = 0$ and a small arbitrary value of $R'(0)$. The solution grows by several thousand orders of magnitude between $r = 0$ and $r = r_c$. To cope with this variation, we included a subroutine to rescale the solution whenever $R(r)$ or its derivatives exceeded some maximum value, typically 10^{30} . Once a solution had been found the boundary condition at $r = r_c$, given by equation (27), was matched by scaling the entire function. Such arbitrary rescalings are valid because of the homogeneous nature of the governing ODE and the zero boundary condition at $r = 0$. In order to calculate the diffusivity field we employed the approximation of Wendell, Van Horn & Sargent (1987) for the electrical conductivity. In addition we needed to calculate the opacity for the given temperature and density. This was done with the data tables and subroutines of the STARS stellar evolution code (Eggleton, Faulkner & Flannery 1973; Pols et al. 1995). In all simulations we have used a CO WD composition for the DC.

The time evolution of the magnetic field following the dispersal of the external field was calculated with a first order Euler finite step method. The code was run multiple times with a variety of step sizes and spatial resolutions with no significant variation in the solution between runs. The induction equation was simplified by the relations

$$\tilde{R}(r) = R(r) + \frac{r}{2} \frac{\partial R}{\partial r}, \quad (30)$$

and

$$R(r) = \frac{1}{r^2} \int_0^r 2r \tilde{R}(r) dr. \quad (31)$$

This removes the spherical geometry of the induction equation, reducing it to the form

$$\frac{\partial \tilde{R}}{\partial t} = \eta \frac{\partial^2 \tilde{R}}{\partial r^2}, \quad (32)$$

which has a zero boundary condition at $r = r_c$ in the absence of an external field and is ultimately easier to work with. The function R and subsequently \mathbf{B} are then recovered from \tilde{R} with the relation in equation (31) numerically evaluated with the trapezoidal rule. The routine does not take into account DC cooling. This is unlikely to affect the evolution of the field during the CE phase and shortly after when the field is evolving rapidly. In the late time evolution however when the field has finished its radial redistribution and is decaying purely exponentially, Wendell, Van Horn & Sargent (1987) showed that the cooling significantly increases the decay timescale and the magnetic field becomes essentially frozen into the dwarf. Therefore we may take the final value for the field strength shortly after it has reached a state of exponential decay. This is typically around 10^7 yr after the dispersion of the CE.

5 RESULTS

The magnetic field produced by the CE is heavily dependent on several key factors. Although the magnetic field of the DC and the CE is continuous at the surface, the total magnetic flux able to penetrate the DC depends on the lifetime of the CE. Once the CE has dispersed, the field continues to migrate inwards and the surface field strength to decay. The degree to which this happens depends on how much of the field is able to penetrate the DC while the surface field is still maintained. This requires a suitable treatment of the radial conductivity profile of the DC. As the density increases towards the centre of the DC the conductivity rises rapidly, inhibiting further diffusion of the field. This results in the confinement of the field to around the outer 10 per cent of the DC by radius.

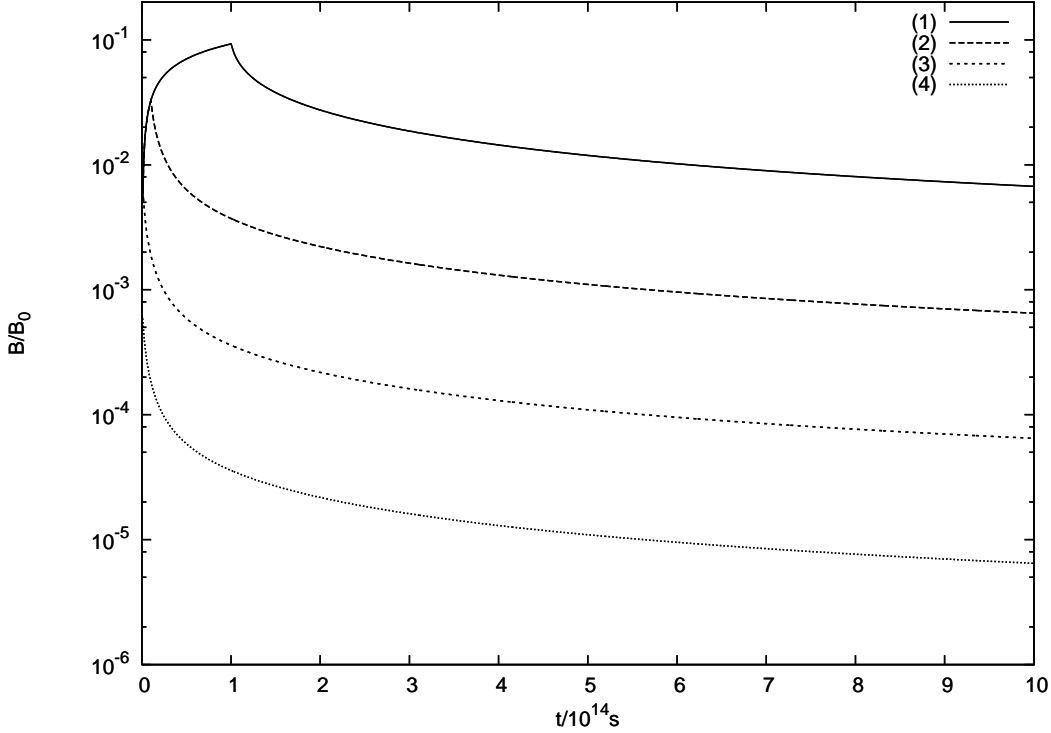


Figure 1. The radial magnetic field strength at $r = 0.99 r_c$ that results from a constant, uniform, vertical magnetic field applied to a DC for (1) 10^{11} s, (2) 10^{12} s, (3) 10^{13} s, (4) 10^{14} s. Note the peak of the field strength at the end of the phase where the external field is applied. After the removal of the external field there is a period of rapid decay lasting around 2×10^{14} s after which the field decays much more slowly on a timescale of around 10^{15} s. The strength of the field is roughly proportional to the lifetime of the external field.

The structure and orientation of the magnetic field of the CE is also of critical importance. In a convectively driven magnetic dynamo we might expect the orientation of the field to change rapidly. The frequency of the changes has important consequences for the field. Given the geometry of the system driving the fluid motions which in turn give rise to the magnetic dynamo we might also anticipate a preferred direction to the orientation of the field. A field that is maintained in a single direction produces a WD field several orders in magnitude stronger than one in which the orientation varies rapidly and with random orientation.

5.1 Consequences of CE lifetime

The lifetime of the CE has a complicated relationship to the original orbital separation of the binary system, the size of the envelope and the properties of the degenerate core and its companion. This is to be expected because of the wide range of magnetic field strengths in MWDs. Here we consider how quickly a field may be built up in the DC as a result of an applied uniform constant vertical magnetic field outside. This mechanism produces stronger magnetic fields than one with varying orientation but it is the best case scenario and places an upper bound on how much field might be retained. While the MHD properties of CEs are not understood, it is difficult to say to what degree there may be a preferred orientation for the magnetic field so the true physical system may resemble anything in between a uni-directional field and one that reorients itself randomly in any direction.

We applied a constant external field of B_0 to a DC of radius $0.01 R_\odot$, mass $0.6 M_\odot$ with diffusivity profile determined by a polytropic index of $3/2$ and temperature 10^5 K. The equations for electrical conductivity from Wendell, Van Horn & Sargent (1987) are not strongly temperature dependent in the highly degenerate density regime. As such, the diffusivity profile for WDs of temperatures varying between 10^3 K and 10^7 K only show noticeable differences at the surface. This has no significant effect on the evolution of the DC field in our model. The magnetic field of the WD scales linearly with the applied field. We tested the cases where the field was applied for 10^{11} s, 10^{12} s, 10^{13} s and 10^{14} s. The radial and meridional fields at $r = 0.99 r_c$ and $r = 0.9 r_c$ are shown in figures 1 to 4. For $r = 0.99 r_c$ we note the two distinct phases of the solution. First there is the initial growth phase in the presence of the external field. Once the external field is removed the field strength peaks and begins to decay. The strength of the field that remains after the removal of the external field increases in proportion to the lifetime of the external field. Following the removal of the external field, the surface field of the exposed WD decays rapidly for around 10^{14} s before continuing to decay exponentially with a characteristic timescale of around 10^{15} s. Whilst this rate of

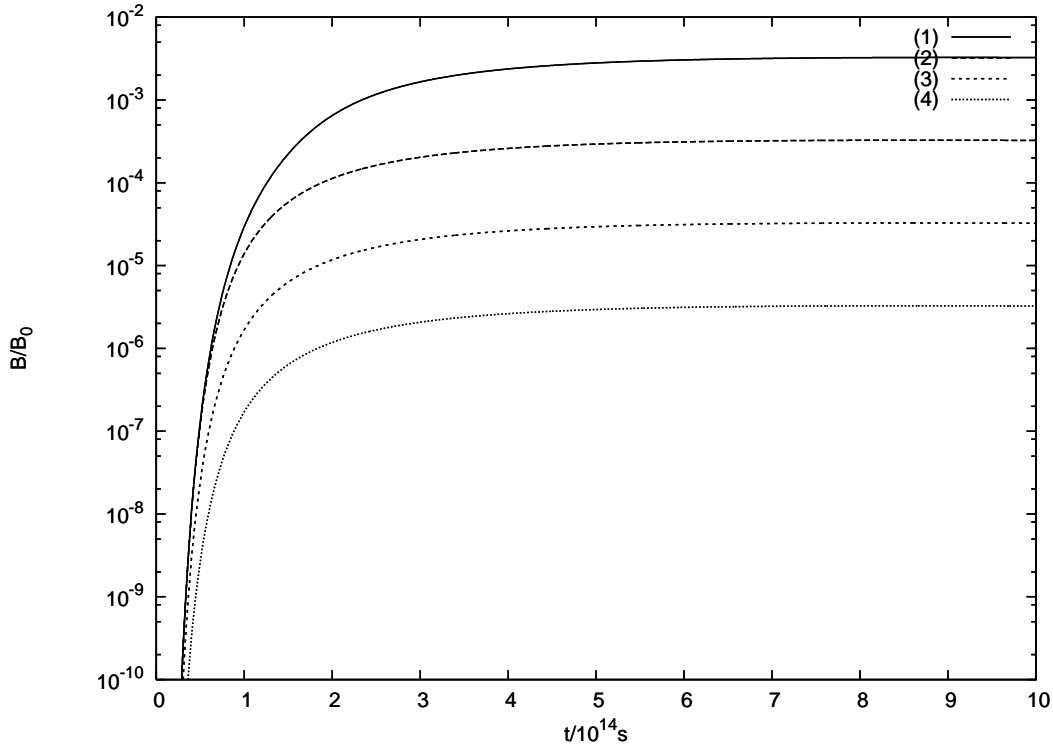


Figure 2. The radial magnetic field strength at $r = 0.9 r_c$ that results from a constant, uniform, vertical magnetic field applied to a DC for (1) 10^{11} s, (2) 10^{12} s, (3) 10^{13} s, (4) 10^{14} s. The magnetic field does not exhibit the same peaks as at $r = 0.99 r_c$ because the saturation of the field takes significantly longer than closer to the surface. The field here continues to grow even after the rapid decay phase of the field closer to the surface as it continues to diffuse inwards. We also see that the strength of the field is roughly proportional to the lifetime of the external field.

decay is too rapid to explain the existence of long-lived WD magnetic fields, our simulations have not included WD cooling. The results of Wendell, Van Horn & Sargent (1987) indicate that cooling causes the diffusivity to decrease and significantly extends the decay time scale for the magnetic field. This effectively freezes the field. If we suppose the magnetic field is frozen after 2×10^{14} s when the field has relaxed to its post CE state then the residual magnetic field strength produced by an external field of strength B_{ext} with lifetime t_{CE} , taking into account both radial and meridional components, is approximately

$$B_{\text{res}} = B_{\text{ext}} \frac{5 t_{\text{CE}} \times 10^{-16}}{\text{s}}. \quad (33)$$

From the results at $r = 0.9 r_c$ we see that the field continues to diffuse inwards after the removal of the external field until it reaches saturation point. This is because the diffusivity decreases towards the interior of the WD. Once the field reaches a certain point, the diffusion becomes so slow that it is effectively halted. This is extremely important if we wish to build strong surface fields because it prevents any further redistribution of magnetic energy. If we look at the magnetic field further into the star we see that the field doesn't penetrate any deeper than $r = 0.5 r_c$ after 10^{15} s and the field inside $r = 0.9 r_c$ is extremely weak compared to the surface field.

5.2 Effect of randomly varying magnetic field orientation

If the direction of the applied field is not constant, as we might expect from a dynamo driven field, then typically the final field strength is reduced by some factor based on the degree of variation. For a spatially constant conductivity with oscillating boundary conditions we may solve the induction equation analytically. This gives us some insight into the mechanisms preventing the build up of strong fields in the case of a rapidly varying external field. We also simulated the change in orientation numerically by taking the field generated by applying a magnetic field for a short time in a single orientation and then taking the sum of the same field rotated at random angles at each timestep up until the dispersion of the CE.

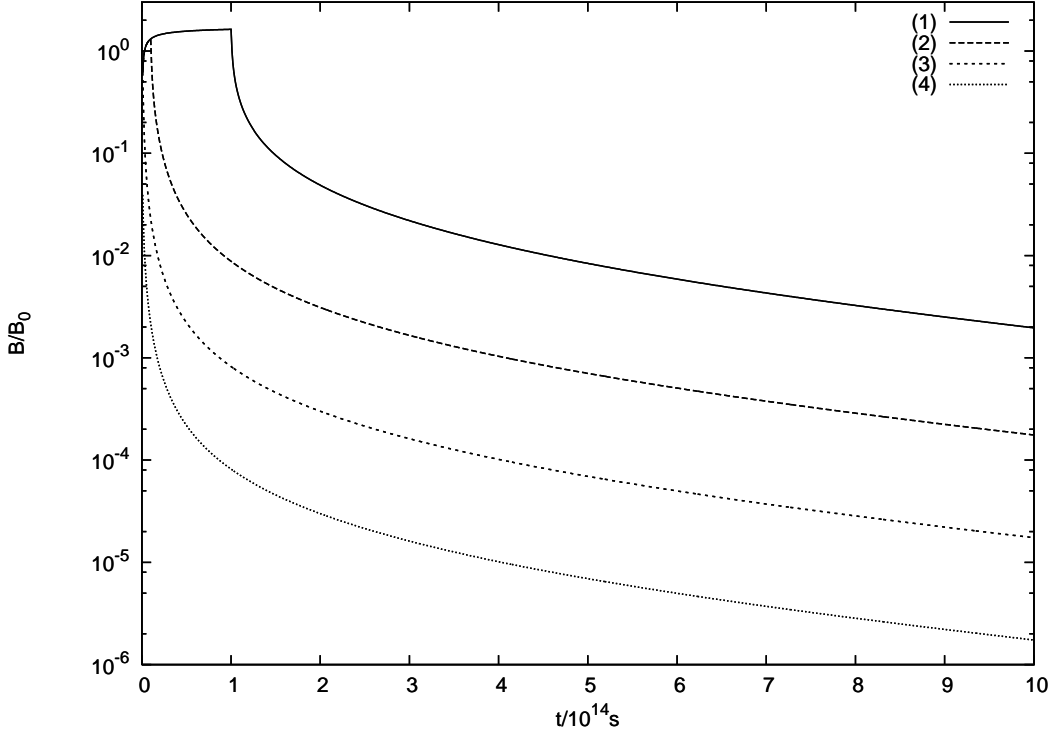


Figure 3. The meridional magnetic field strength at $r = 0.99 r_c$ that results from a constant, uniform, vertical magnetic field applied to a DC for (1) 10^{11} s, (2) 10^{12} s, (3) 10^{13} s, (4) 10^{14} s. Note the peak of the field strength at the end of the phase where the external field is applied. After the removal of the external field there is a period of rapid decay lasting around 2×10^{14} s after which the field decays much more slowly on a timescale of around 10^{15} s. The strength of the meridional field is several orders of magnitude larger than the radial field. The strength of the field is roughly proportional to the lifetime of the external field.

5.2.1 Uniform diffusivity DC

In the case where η_r is a constant we are able to solve for R analytically as in section 3. In this case, $\eta(t) = \eta_r \eta_t(t)$ and equation (23) becomes the Helmholtz equation and we seek solutions in the form of spherical Bessel functions. We find that $R \propto j_1 \left((i\gamma)^{\frac{1}{2}} r \right)$. Then from equations (28) and (21) we find

$$S = \frac{3}{4} \int_{-\infty}^{\infty} \hat{B}_z(\gamma) \left(\frac{j_1 \left((i\gamma)^{\frac{1}{2}} r \right)}{j_1 \left((i\gamma)^{\frac{1}{2}} r_c \right) + \frac{1}{2} (i\gamma)^{\frac{1}{2}} j_1' \left((i\gamma)^{\frac{1}{2}} r_c \right)} \right) e^{i\gamma H} d\gamma \cos \theta. \quad (34)$$

Consider the strength of the field generated at the surface of the DC by each γ -mode. We define $Q(\gamma)$ by

$$Q(\gamma) = \text{Re} \left[\frac{j_1 \left((i\gamma)^{\frac{1}{2}} r_c \right)}{j_1 \left((i\gamma)^{\frac{1}{2}} r_c \right) + \frac{1}{2} (i\gamma)^{\frac{1}{2}} j_1' \left((i\gamma)^{\frac{1}{2}} r_c \right)} \right]. \quad (35)$$

We shall refer to $Q(\gamma)$ as the transfer efficiency because it represents roughly the radial magnetic flux across the surface of the DC relative to the imposed field. Fig. 5 shows how $Q(\gamma)$ varies. We see that for $\gamma > 1$, $Q(\gamma)$ falls off approximately as $\gamma^{-\frac{1}{2}}$. So the higher γ modes of the system are more effectively suppressed but the fall off is slow. This means that the radial magnetic field at the surface of the star for very large γ approaches 0. In this case the boundary conditions are matched by the dipolar field which cancels out the imposed field at the surface of the DC. We can see this by evaluating the term in the integrand of equation 26 at $r = r_c$ for a specific value of γ . The term tends to -2 as $\gamma \rightarrow \infty$. This is exactly what is required to cancel the imposed field.

If we consider a system with constant diffusivity η , then $H = \eta t$. If we then take $B_z(t) \propto \cos(\alpha t)$ it is easy to show that the transfer efficiency is $Q(\frac{\alpha}{\eta})$. We interpret this by recognising that, if the rate of oscillation is too high compared to the diffusivity each time the external field switches, most of the field generated by the previous oscillation is cancelled out. If the diffusivity is high enough, the oscillations are less effectively cancelled and a residual field is able to build up.

Now let us consider the radial form of the induced field. From our discussion above we expect that the field is functionally similar to $\text{Re}[j_1(i\alpha/\eta)^{1/2} r]$. Fig. 6 shows the form of the field that results from this solution (equations 5, 27 and 29). We have

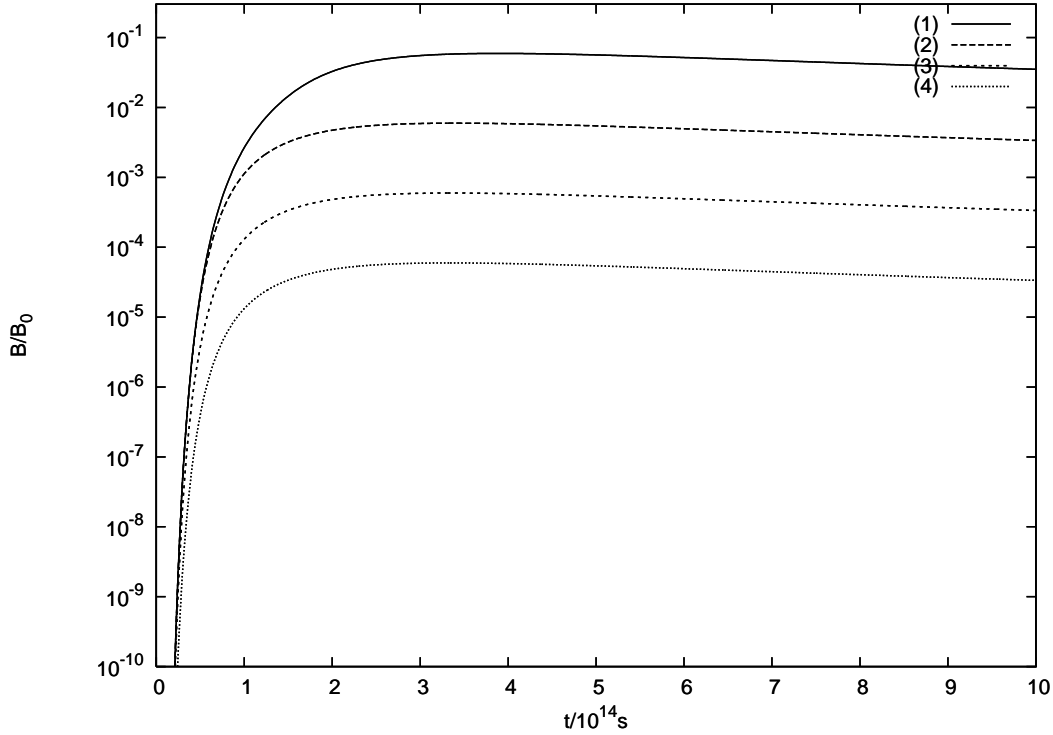


Figure 4. The meridional magnetic field strength at $r = 0.9 r_c$ that results from a constant, uniform, vertical magnetic field applied to a DC for (1) 10^{11} s, (2) 10^{12} s, (3) 10^{13} s, (4) 10^{14} s. The magnetic field does not exhibit the same peaks as at $r = 0.99 r_c$ because the saturation of the field takes significantly longer than closer to the surface. The field here continues to grow even after the rapid decay phase of the field closer to the surface as it continues to diffuse inwards. We also see that the strength of the field is roughly proportional to the lifetime of the external field.

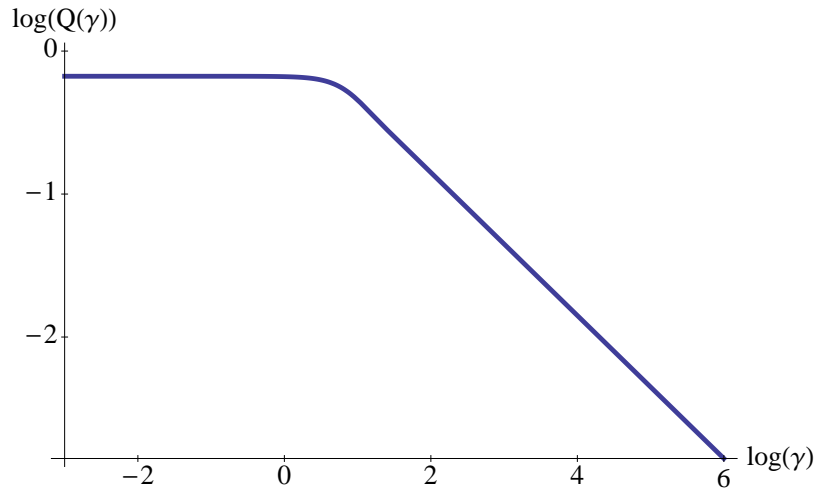


Figure 5. Behaviour of the transfer efficiency factor, $Q(\gamma)$ as described in section 5.2.1.

used the parameters given above and an imposed field strength of B_0 . So, although the transfer efficiency is very low and the radial field is suppressed, the strong R gradient produces an internal field parallel to the surface which is comparable in magnitude to the imposed field but decays extremely rapidly with depth. The thickness of this layer behaves asymptotically as $(\frac{a}{\eta})^{-1/2}$. We note that this is the same behaviour as the efficiency factor $Q(\gamma)$. This is reasonable because the efficiency of transfer of magnetic energy from the external field to the DC should scale roughly in proportion to how far the field can penetrate, at least for shallow layers.

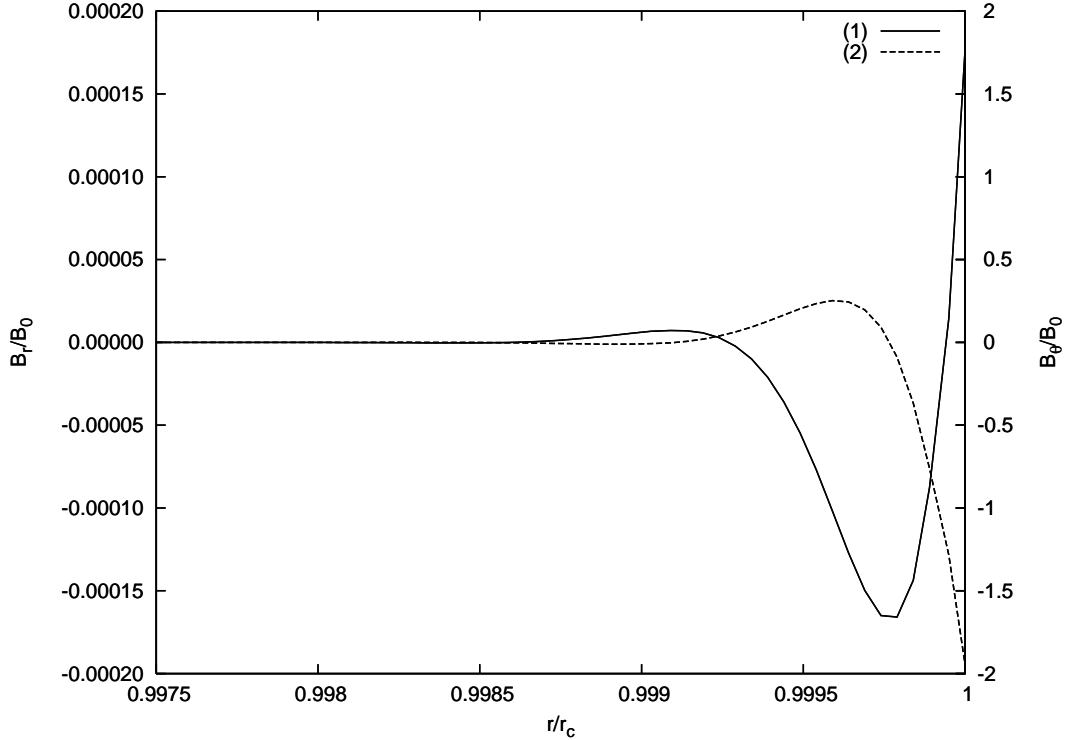


Figure 6. Form of the induced field within the DC with a spatially uniform magnetic diffusivity $\eta = 221\text{cm}^2\text{s}^{-1}$ with variation frequency $\alpha = 2 \times 10^{-8}\text{s}^{-1}$ for an imposed field of B_0 . (1) Radial field (B_r), (2) Meridional field (B_θ). We see from the horizontal axis that the field is confined to the most outer regions of the DC. This is because the rapid variation of the external field causes any field that is generated at the surface to smooth out to zero as it diffuses inwards. We also see that the meridional field is several orders of magnitude stronger than the radial field.

Because we are proposing a model in which the magnetic field of a common envelope surrounding a binary system induces the magnetic field of the DC we choose a value of α to reflect this. First consider a far-field varying on a time scale similar to the orbital period of the binary system. We determine this time scale for a $0.6 M_\odot$ DC with a typical red giant companion of mass $6 M_\odot$ and radius $400 R_\odot$ which has filled its Roche Lobe. This gives us an orbital time scale of $t_{\text{orbit}} \approx 3.5 \times 10^8\text{s}$ and so we choose $\alpha = \frac{2\pi}{t_{\text{orbit}}} \approx 2 \times 10^{-8}\text{s}^{-1}$. This gives a transfer efficiency of $Q(\frac{\alpha}{\eta}) \approx 2 \times 10^{-4}$. Alternatively as we suggested earlier, the magnetic dynamo is likely to be stronger when the orbit of the binary has decayed. If we apply the same analysis with $t_{\text{orbit}} = 1\text{day}$ then $Q \approx 4 \times 10^{-6}$. In either case, the field is still confined to a very thin boundary layer and is almost entirely meridional.

5.2.2 Post CE evolution of the magnetic field

Following the initial generation of the magnetic field within the DC we foresee two possible cases for the subsequent evolution. Either the CE is dispersed on a time scale shorter than the variation of magnetic diffusivity or the diffusivity varies by a significant factor over the lifetime of the CE. In the absence of a magnetic field, the lifetime of the CE phase is estimated on the order of 10^3yr (Taam, Bodenheimer & Ostriker 1978). The time scale for orbital decay as a result of a dynamo driven wind is estimated to be a few Myr (Regö s & Tout 1995). If energy from orbital decay is transformed to magnetic energy rather than unbinding the envelope then the lifetime of the CE phase is prolonged though from the energy considerations of section 2 the lifetime is likely to lie much closer to the lower bound. Depending on the degree to which this happens the lifetime of the dynamo may lie anywhere between these two bounds. Typically the diffusivity varies on a time scale of $t_\eta \approx 10^{16}\text{s} \approx 3 \times 10^{10}\text{yr}$, much longer than the probable lifetime of the CE. However our understanding of CE evolution is sufficiently poor that these estimates may bear little resemblance to reality.

The decay of an unsupported magnetic field occurs on a time scale $t_B \approx \beta \frac{r_c^2}{\eta}$ where β is a constant related to the field geometry. For an unsupported field, $\beta = \pi^2$. In the case where $\eta = 221\text{cm}^2\text{s}^{-1}$ which is a good approximation for the surface layers of a DC and $r_c = 0.01 R_\odot$ we get $t_B \approx 2\beta \times 10^{15}\text{s}$. Wendell, Van Horn & Sargent (1987) showed that the magnetic field of a WD without an imposed field has a decay time which is much longer than the evolutionary age of the WD over its whole lifetime and so the magnetic field is essentially frozen into the WD. We observe that, in our setup where the internal field is supported by a rapidly oscillating external field, the strong confinement of the field to the outermost layers of the DC

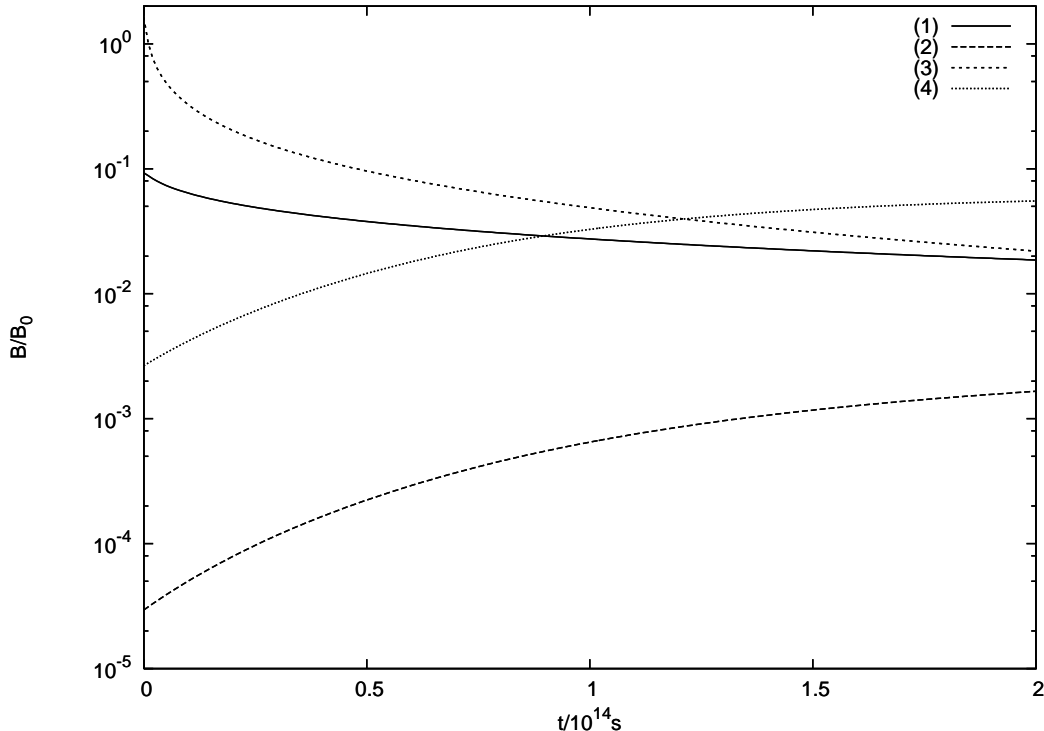


Figure 7. Decay of the magnetic field of a WD upon removal of a constant external magnetic field applied for 10^{14} s. (1) $B_r(r = 0.99 r_c)$ (2) $B_r(r = 0.9 r_c)$, (3) $B_\theta(r = 0.99 r_c)$, (4) $B_\theta(r = 0.9 r_c)$. Although the surface meridional field is initially much stronger than the radial field it decays much faster until the two are roughly equal 2×10^{14} s after the external field is removed. We also see that, even after the rapid initial decay of the surface field seems to have finished, the field at $0.9 r_0$ is still growing as the field diffuses inwards.

produces strong gradients which lead to rapid magnetic diffusion. Once the field is removed, the system rapidly relaxes to the solution given by zero external field. The field then decays on an ohmic time scale of t_B with $\beta = \pi^2$ (Proctor & Gilbert 1994).

Fig. 7 shows the evolution of the field produced by a DC with diffusivity profile determined from a polytropic structure. The field strengths of the radial and meridional fields are shown at $r/r_c = 0.99$ and 0.9 . We see that, once the external field vanishes, the field spreads slowly inwards. The field was calculated below $r/r_c = 0.9$ but even by the end of the simulation, no field had reached as deep as $r/r_c = 0.5$. The surface magnetic field decays by about a factor of 10^2 as it relaxes owing to the redistribution of the magnetic energy over the radius. This occurs on a time scale of around 2×10^{13} s. After the initial rapid decay, the surface field continues to decay exponentially on a much longer timescale of around 10^{14} s. This is faster than predicted analytically but as Fig. 7 shows the field at $r/r_c = 0.9$ is still growing so the system has not fully relaxed. It is likely that the decay timescale grows as the field moves towards spatial equilibrium. WD cooling which has not been included here would also prevent additional decay.

We have neglected secondary effects that are produced as a result of the finite time the magnetic dynamo of the CE takes to decay. We expect though, given that the lifetime of the CE is estimated to be significantly shorter than the relaxation time for the field, the magnetic dynamo is likely to decay on an even shorter time scale. Thus the effect on the solution should be negligible.

5.2.3 Numerically evolved field with random orientation

In order to simulate a randomly varying external field in a more three-dimensional sense we considered a supposition of multiple copies of a base field rotated into random orientations applied in sequence. The base field was generated by applying a constant vertical field for a range of times much shorter than the lifetime of the CE. Such a superposition is valid because the induction equation is linear. So if the field generated by applying a constant vertical magnetic field for time δt is $\tilde{\mathbf{B}}(t)$ then the total field is

$$\mathbf{B}(t) = \sum_{k=1}^N \mathbf{n}_k \times \tilde{\mathbf{B}}(t + k\delta t), \quad (36)$$

where \mathbf{n}_i are randomly generated vectors and $N\delta t$ is the duration of the magnetic dynamo. The results are shown in Table 1.

t_{dyn}/s	B_{R}/G	B_{M}/G	B_{T}/G
No preferred orientation			
10^6	1.9×10^{-6}	-1.8×10^{-6}	1.3×10^{-5}
10^7	-3.3×10^{-6}	4.0×10^{-7}	-4.1×10^{-6}
10^8	-3.6×10^{-6}	-2.6×10^{-6}	-1.6×10^{-6}
10^9	4.2×10^{-5}	-1.6×10^{-5}	3.9×10^{-6}
Half-plane restricted orientation			
10^6	2.3×10^{-3}	-4.2×10^{-6}	-1.1×10^{-5}
10^7	2.9×10^{-3}	-2.5×10^{-6}	3.8×10^{-6}
10^8	1.9×10^{-3}	-9.2×10^{-6}	8.7×10^{-6}
10^9	2.0×10^{-3}	1.6×10^{-5}	1.4×10^{-5}

Table 1. Residual surface magnetic field strengths generated by an external field of unit strength which reorients at intervals of t_{dyn} . B_{R} is the radial field, B_{M} is the meridional field and B_{T} is the toroidal field. The external field lasts for a total of 10^{13} s and the residual field is taken at 2×10^{14} s

t_{CE}/s	B_{R}/B_0	B_{M}/B_0	B_{T}/B_0
No preferred orientation			
10^{11}	4.7×10^{-6}	1.8×10^{-6}	4.0×10^{-7}
10^{12}	3.2×10^{-6}	-4.8×10^{-6}	-8.5×10^{-7}
10^{13}	4.2×10^{-5}	-1.6×10^{-5}	3.9×10^{-6}
10^{14}	-6.7×10^{-5}	-3.3×10^{-5}	-4.9×10^{-5}
Half-plane restricted orientation			
10^{11}	1.9×10^{-5}	3.0×10^{-7}	2.8×10^{-6}
10^{12}	2.0×10^{-4}	1.1×10^{-6}	1.5×10^{-5}
10^{13}	2.0×10^{-3}	-2.3×10^{-5}	1.3×10^{-5}
10^{14}	3.1×10^{-2}	-1.2×10^{-4}	9.5×10^{-5}

Table 2. Residual surface magnetic field strengths generated by an external field of strength B_0 which reorients at intervals of 10^9 s. B_{R} is the radial field, B_{M} is the meridional field and B_{T} is the toroidal field. The external field lasts for t_{CE} and the residual field is taken at 2×10^{14} s

We find that in the case of a purely random orientation, the residual field is smaller than the constant external field case by a factor of around 1000. This is to be expected because, on average, each field orientation is opposed by one pointing in the opposite direction. The fluctuations arise from the random nature of the field orientation and the different times at which each field is applied. It seems certain that the magnetic field strength that would be needed to generate observed magnetic fields would be extremely large in this case.

5.2.4 Effect of introducing a preferred direction to the external field

Due to the nature of the proposed magnetic dynamo it seems reasonable to suggest that there may be a preferred direction to the magnetic field. If the field is generated by perturbations in the CE owing to the orbital motion of the DC and its companion, the magnetic field lines may show a tendency to align with the orbit. This contrasts with the dynamo mechanism in accretion discs which is a result of the magneto-rotational instability producing eddies that have no preferred direction. Therefore we restrict the magnetic field vector to lie within a hemisphere. The results are also included in Table 1. We find that the residual radial field can now reach strengths close to those produced by the constant external field. This does not apply to the meridional field or the toroidal field because different orientations may still oppose each other and give typically weak field strengths.

If we now vary the CE lifetimes (Table 2) we see that in the case of purely random orientations, the overall field strength is largely unaffected by changes in the CE lifetime. In the case where the field has preferred alignment, the residual radial field strength increases roughly linearly with CE lifetime as in the case of constant external field. It is also able to produce fields with similar field strength to the uni-directional case. This suggests that while dynamo action may result in fluctuating magnetic field orientations with time, the residual field strength can be maintained provided that the dynamo has a preferred direction on average.

6 CONCLUSIONS & DISCUSSION

The statistical occurrence of magnetic WDs in close interacting binary systems suggests that the origin of their strong fields is a product of some feature of their binary evolution. Indeed, the argument that the fields originate through flux conservation during the collapse of Ap/Bp stars does not explain the higher frequency in interacting binaries. By building on the proposal

that the magnetic field is generated by dynamo action within a common convective envelope we have shown that strong fields may be transferred to the DC. These fields can then be preserved upon dissipation of the envelope.

Following the dissipation of the CE, we have found that the system rapidly relaxes on a timescale of about 7 Myr to the state we would anticipate given no external field. Although there is no significant dissipation of magnetic energy during this time, the redistribution of magnetic flux towards the interior of the WD results in significant decay of the surface field by around a factor of at least 10–100. Further decay is prevented by the increasing electrical conductivity towards the interior of the WD. This prevents field diffusing beyond around $r = 0.9r_c$. Once the field has relaxed to its new configuration it continues to decay but on a timescale much longer than the time scale for cooling of the WD so we expect any further loss of field strength to be minimal.

The maximal rate of transfer of field energy from the CE to the DC occurs when the field is kept fixed. In this case the residual strength of the field following dissipation of the CE is linearly related to the lifetime of the CE. If we combine equations (8) and (33) we find

$$M = 5.7 \times 10^{35} \left(\frac{B_{\text{res}}}{10^7 \text{ G}} \right)^2 \left(\frac{a}{0.01 \text{ au}} \right) \left(\frac{r_1}{0.01 R_{\odot}} \right)^2 \left(\frac{t_{\text{CE}}}{2 \times 10^{15} \text{ s}} \right)^{-2} \text{ J.} \quad (37)$$

If we assume that all of the energy released through orbital decay is transformed into magnetic energy then this requires an envelope lifetime of $1.1 \times 10^{12} \text{ s}$ or $3.6 \times 10^4 \text{ yr}$ to produce a 10^7 G magnetic field. This lifetime is extended if there is variation in the direction of the field produced by the dynamo or there are energy sinks other than the magnetic field. Because the required envelope lifetime scales linearly with B_{res} , weaker fields could be produced on a much shorter time scale. Energetically there is nothing to prevent formation of a 10^9 G MWD. As shown, the final field strength scales proportionally with the CE lifetime. If the dynamo is confined to a smaller region or the CE lifetime is extended then this strength of field could be produced. Scenarios this extreme seem unlikely and this is complemented by the rarity of MWDs with such strong magnetic fields. We do not rule out the possibility that the strongest fields may be produced by the merger of a white dwarf and the core of a giant star which have both been strongly magnetized during CE phases.

We have also shown that the production of sufficiently strong fields is almost certainly dependent on some preferred orientation of the magnetic dynamo. In the case where there is no preferred direction the DC magnetic field is confined to a layer of thickness about $(\frac{\alpha}{\eta})^{-1/2}$, where α is the frequency for field variation, and is almost entirely meridional. Despite the generation of strong surface fields during the CE phase in this case, the total magnetic energy of the DC field is constrained by the depth of the magnetic layer. Consequently once the CE disperses and the field of the exposed WD begins to diffuse inwards, the majority of the field strength is lost. This result is confirmed by the numerical simulations. Typically a field strength of 10^{-5} relative to the average magnetic field strength of the dynamo is the largest possible residual field. This may be sufficient to produce WDs with weaker fields but the formation of the strongest WD magnetic fields would require far more energy than the system could provide. In the case where the field has some preferred orientation, the proportion of field retained is increased up to a few per cent depending on the lifetime of the CE dynamo.

Whilst the arguments we have presented here suggest that the origin of the fields of MWDs may be the result of dynamo action in CEs of closely interacting binaries, there are still many uncertainties. Most of these are the result of insufficient understanding of the formation and evolution of CEs. The field structures we have used to construct our models are simple but complex field geometries are observed in WDs such as Feige 7 and KPD 0253+5052. If CE dynamos are responsible for the origins of MWDs, they should support complex geometries. Further progress depends on a better understanding of the physical processes and energy transfer within the CE.

ACKNOWLEDGEMENTS

This work was supported by the STFC.

REFERENCES

- Chanmugam G., 1992, ARA&A, 90, 143
 Eggleton P. P., Faulkner J., Flannery, B. P., 1973, A&A 23, 325
 Gänsicke B. T., Long S. K., Barstow M. A., Hubeny I., 2006, ApJ, 639, 1039
 Hubbard W. B., Lampe M., 1969, ApJS, 163, 18, 297
 Kafka S., Honeycutt R. K., Howell S. B., Harrison T. E., 2005, AJ, 130, 2852
 Landstreet J. D., Angel J. R. P., 1971, in Davies R. D., Graham-Smith F., eds, Proc. IAU Symp 46, The Crab Nebula. Reidel, Dordrecht, p. 234
 Liebert J., Wickramasinghe D. T., Schmidt G. D. et al., 2005, AJ, 129, 2376
 Livio M., Soker N., 1988, ApJ, 329, 764

- Meyer F., Meyer-Hofmeister E., 1979, *A&A*, 78, 167
- Nelemans G., Verbunt F., Yungelson L. R., Portegies Zwart S. F., 2000, *A&A*, 360, 1011
- Paczýński B., 1976, in Eggleton P. P., Mitton S., Whelan J., eds, *Proc. IAU Symp. 73, Structure and Evolution of Close Binary Systems*. Reidel, Dordrecht, p. 75
- Paczýński B., Ziółkowski J., 1967, *Acta Astron.*, 17, 7
- Pols O., Tout C. A., Eggleton P. P., Han Z., 1995, *MNRAS* 274, 964
- Press W. H., Teukolsky S. A., Vetterling W. T., Flannery B. P., 1992, *Numerical Recipes in Fortran 77, Second Edition*. Cambridge Univ. Press, Cambridge
- Proctor M. R. E., Gilbert A. D., 1994, *Lectures on Solar and Planetary Dynamos*. Cambridge Univ. Press, Cambridge
- Regós E., Tout C. A., 1995, *MNRAS*, 273, 146
- Schmidt G. D., Harris H. C., Liebert J. et al., 2003, *ApJ*, 595, 1101
- Silvestri N. M., Lemagie M. P., Hawley S. L. et al., 2007, *AJ*, 134, 741
- Southwell K. A., Still M. D., Smith R. C., Martin J. S., 1995, *A&A* 302, 90
- Taam R. E., Bodenheimer P., Ostriker J. P., 1978, *ApJ*, 222, 269
- Tout C. A., Pringle J. E., 1992, *MNRAS*, 256, 269
- Tout C. A., Wickramasinghe D. T., Liebert J., Ferrario L., Pringle J. E., 2008, *MNRAS*, 387, 897
- Valyavin G., Bagnulo S., Fabrika S., Reisenegger A., Wade G. A., Han I., Monin D., 2006, *ApJ*, 648, 559
- Webbink R. F., 1976, *ApJ*, 209, 829
- Webbink R. F., 2008, in Milone E. F., Leahy D. A., Hobill D. W., eds, *Short-Period Binary Stars: Observations, Analyses, and Results*. Springer, Berlin, p. 233
- Wendell C. E., Van Horn H. M., Sargent D., 1987, *ApJ*, 313, 284
- Wickramasinghe D. T., Ferrario L., 2000, *PASP*, 112, 873
- Wickramasinghe D. T., Martin B., 1985, *MNRAS*, 212, 353
- Yakovlev D. G., Urpin V. A., 1980, *Soviet Astr.*, 24, 303